

Stochastic modeling of scalar dissipation rate fluctuations in non-premixed turbulent combustion

By Heinz Pitsch AND Sergei Fedotov†

1. Motivation and objectives

In non-premixed combustion chemical reactions take place when fuel and oxidizer mix on a molecular level. The rate of molecular mixing can be expressed by the scalar dissipation rate, which is for the mixture fraction Z defined as

$$\chi = 2D_Z (\nabla Z)^2, \quad (1.1)$$

where D_Z is the diffusion coefficient of the mixture fraction. The scalar dissipation rate appears in many models for turbulent non-premixed combustion as, for instance, the flamelet model (Peters (1984), Peters (1987)), the Conditional Moment Closure (CMC) model (Klimenko & Bilger (1999)), or the compositional pdf model (O'Brien (1980), Pope (1985)). In common technical applications, it has been found that if the scalar dissipation rates are much lower than the extinction limit, fluctuations of this quantity caused by the turbulence do not influence the combustion process (Kuznetsov & Sabel'nikov (1990), Pitsch & Steiner (2000)). However, it has been concluded from many experimental (Saitoh & Otsuka (1976)) and theoretical studies (Haworth *et al.* (1988), Mauss *et al.* (1990), Barlow & Chen (1992), Pitsch *et al.* (1995)) that there is a strong influence of these fluctuations if conditions close to extinction or auto-ignition are considered. For instance, in a system where the scalar dissipation rate is high enough to prohibit ignition, random fluctuations might lead to rare events with scalar dissipation rates lower than the ignition limit, which could cause the transition of the whole system to a burning state.

In this study, we investigate the influence of random scalar dissipation rate fluctuations in non-premixed combustion problems using the unsteady flamelet equations. These equations include the influence of the scalar dissipation rate and have also been shown to provide very reasonable predictions for non-premixed turbulent combustion in a variety of technical applications (Pitsch *et al.* (1996), Pitsch *et al.* (1998), Barths *et al.* (1998)). However, it is clear that these equations are actually not capable of describing all of the features which might occur in turbulent non-premixed flames. For instance, in jet diffusion flames, local extinction events might occur close to the nozzle because of high scalar dissipation rates. These extinguished spots might reignite downstream, not by auto-ignition, but by heat conduction and diffusive mass exchange with the still burning surroundings. It should be kept in mind that the motivation in this work is not to predict actual turbulent reacting flows, but to study the dynamical system defined by the equations described in the following section. The advantage of the present simplified approach allows a study of the extinction process isolated from auto-ignition and re-ignition events.

† UMIST, Manchester, England

The basic purpose of this paper is to analyze how random fluctuations of the scalar dissipation rate can affect extinction of non-premixed combustible systems. The approach, based on stochastic differential equations, allows us to take random extinction events into account. In this case the critical conditions must be different from those involving deterministic situations. Here, we look at these phenomena in terms of noise-induced transitions theory, where multiplicative noise of sufficient intensity can drastically change the behavior of a system (Horsthemke & Lefever (1984)). In the present case, the probability density function for the temperature in the reaction zone may undergo qualitative changes as the intensity of random fluctuations increases. It should be noted that a similar analysis has been done in a series of works on the stochastic analysis of thermal ignition of explosive systems in (Buyevich *et al.* (1993), Fedotov (1992), Fedotov (1993)).

Oberlack *et al.* (1999) have investigated the influence of Damköhler number fluctuations in a well-stirred reactor. The fundamental difference compared to the present study is that in a well stirred reactor the mixing process is assumed to be infinitely fast. The Damköhler number, therefore, represents the residence time rather than the mixing time and appears in the non-dimensional chemical source term. Hence, imposing stochastic variations of the Damköhler number corresponds to a fluctuating chemical source term. Here, however, the fluctuating quantity is the scalar dissipation rate, which appears as a diffusion coefficient. The response of the mixing field to this fluctuating diffusion coefficient and the interaction with the chemical source term are investigated. Moreover, in the present formulation we allow for temporal changes of the fluctuating quantity and also consider its pdf.

In this paper, we will first present the non-dimensional flamelet equations for a one-step global reaction. With this assumption the system can be reduced to a single equation for the temperature. We will then derive stochastic differential equations for the temperature and the scalar dissipation rate. These equations lead to a partial differential equation for the joint probability density function of the temperature and the scalar dissipation rate. This equation will be discussed and numerical solutions will be presented.

2. Governing equations

2.1. Flamelet equations

Assuming an irreversible one-step reaction of the form $\nu_F F + \nu_O O \rightarrow P$, where F, O, and P denote fuel, oxidizer, and reaction product, respectively, the flamelet equations for the mass fractions of fuel Y_F , oxidizer Y_O , reaction product Y_P , and the temperature T , can be written as

$$\frac{\partial Y_i}{\partial t} - \frac{\chi}{2} \frac{\partial^2 Y_i}{\partial Z^2} + \nu_i W_i w = 0, \quad i = F, O, P \quad (2.1)$$

$$\frac{\partial T}{\partial t} - \frac{\chi}{2} \frac{\partial^2 T}{\partial Z^2} - \frac{Q}{c_p} w = 0. \quad (2.2)$$

Here, ν_i are the stoichiometric coefficients, W_i the molecular weights, t is the time, ρ the density, c_p the specific heat capacity at constant pressure, and Q is the heat of reaction defined as $Q = -\sum_i \nu_i W_i h_i$, where h_i denotes the enthalpy of species i . The mixture fraction Z is defined as

$$Z = \frac{\hat{\nu} Y_F - Y_O + Y_{O,2}}{\hat{\nu} Y_{F,1} + Y_{O,2}} \quad \text{with} \quad \hat{\nu} = \frac{\nu_O W_O}{\nu_F W_F}, \quad (2.3)$$

where the subscripts 1 and 2 refer to the conditions in the fuel stream and the oxidizer stream, respectively.

The parameter χ appearing in Eqs. (2.1) and (2.2) is the scalar dissipation rate, which has already been defined by Eq. (1.1). The reaction rate per unit mass w is given by

$$w = \rho \frac{Y_F Y_O}{W_F W_O} A \exp\left(-\frac{E}{\mathcal{R}T}\right), \quad (2.4)$$

where A is the frequency factor and E the activation energy of the global reaction, respectively. \mathcal{R} is the universal gas constant.

2.2. Non-dimensionalization

In order to investigate the flamelet equations with respect to the relevant non-dimensional parameters, it is convenient to introduce the non-dimensional temperature θ and mass fractions of fuel y_F , oxidizer y_O , and reaction product y_P as

$$\theta = \frac{T - T_{st,u}}{T_{st,b} - T_{st,u}}, \quad y_F = \frac{Y_F}{Y_{F,st,u}}, \quad y_O = \frac{Y_O}{Y_{O,st,u}}, \quad y_P = (\nu + 1) \frac{\nu_F W_F}{\nu_P W_P} \frac{Y_P}{Y_{F,1}}, \quad (2.5)$$

where the index st refers to stoichiometric conditions and the unburnt values of temperature, fuel, and oxidizer at stoichiometric conditions are given by

$$T_{st,u} = T_2 + (T_1 - T_2) Z_{st}, \quad Y_{i,st,u} = Y_{i,2} + (Y_{i,1} - Y_{i,2}) Z_{st}, \quad i = F, O. \quad (2.6)$$

The adiabatic temperature for complete conversion of fuel to products is

$$T_{st,b} = T_{st,u} + \frac{L}{c_p}, \quad L = \frac{Y_{F,1} Q}{W_F \nu_F (\nu + 1)} \quad \nu = \dot{\nu} \frac{Y_{F,1}}{Y_{O,2}}. \quad (2.7)$$

With these definitions and Eq. (2.3), the mixture fraction can be expressed as

$$Z = \frac{\nu y_F - y_O + 1}{\nu + 1}, \quad (2.8)$$

from which the stoichiometric mixture fraction

$$Z_{st} = \frac{1}{\nu + 1} \quad (2.9)$$

follows.

The non-dimensional time τ is given by

$$\tau = \frac{\chi_{st,0}}{a} t \quad \text{with} \quad a = 2\Delta Z \cdot Z_{st}(1 - Z_{st}) = \frac{2\Delta Z \nu}{(1 + \nu)^2}, \quad (2.10)$$

where the reference value for the scalar dissipation rate $\chi_{st,0}$ and the parameter ΔZ will be introduced below.

The non-dimensional scalar dissipation rate x , the Damköhler number Da , and the Zeldovich number Ze are defined as

$$x = \frac{\chi}{\chi_{st,0}}, \quad Da = \frac{\nu \nu_F a \rho_{st,u} Y_{O,2}}{(\nu + 1) W_O} \frac{A}{\chi_{st,0}} \exp(-\beta_{ref}) \quad (2.11)$$

$$Ze = \alpha \beta, \quad \alpha = \frac{T_{st,b} - T_u}{T_{st,b}}, \quad \beta = \frac{E}{\mathcal{R}T_{st,b}}. \quad (2.12)$$

With the assumption of constant molecular weight of the mixture, the density ρ can

be expressed in terms of the non-dimensional temperature θ as

$$\rho = \frac{(1 - \alpha)}{1 - \alpha(1 - \theta)} \rho_{\text{st},u}. \quad (2.13)$$

Introducing these definitions into the flamelet equations, Eqs. (2.1) and (2.2), yields

$$\frac{\partial y_{\text{F}}}{\partial \tau} - \frac{ax}{2} \frac{\partial^2 y_{\text{F}}}{\partial Z^2} + \frac{1}{\nu + 1} \omega = 0 \quad (2.14)$$

$$\frac{\partial y_{\text{O}}}{\partial \tau} - \frac{ax}{2} \frac{\partial^2 y_{\text{O}}}{\partial Z^2} + \frac{\nu}{\nu + 1} \omega = 0 \quad (2.15)$$

$$\frac{\partial y_{\text{P}}}{\partial \tau} - \frac{ax}{2} \frac{\partial^2 y_{\text{P}}}{\partial Z^2} - \omega = 0 \quad (2.16)$$

$$\frac{\partial \theta}{\partial \tau} - \frac{ax}{2} \frac{\partial^2 \theta}{\partial Z^2} - \omega = 0, \quad (2.17)$$

where the non-dimensional chemical source term is given by

$$\omega = \text{Da} \frac{(\nu + 1)^2}{\nu} \frac{(1 - \alpha) \exp(\beta_{\text{ref}} - \beta)}{1 - \alpha(1 - \theta)} y_{\text{F}} y_{\text{O}} \exp\left(-Z e \frac{1 - \theta}{1 - \alpha(1 - \theta)}\right). \quad (2.18)$$

The boundary conditions for Eqs. (2.14) – (2.17) are

$$Z = 0 : \quad y_{\text{F},2} = 0, \quad y_{\text{O},2} = 1, \quad y_{\text{P},2} = 0, \quad \theta_2 = 0 \quad (2.19)$$

$$Z = 1 : \quad y_{\text{F},1} = 1, \quad y_{\text{O},1} = 0, \quad y_{\text{P},1} = 0, \quad \theta_1 = 0. \quad (2.20)$$

2.3. Coupling functions

Adding Eqs. (2.14), (2.15), and (2.17) yields a conservation equation for $y_{\text{F}} + y_{\text{O}} + \theta$ as

$$\frac{\partial}{\partial \tau} (y_{\text{F}} + y_{\text{O}} + \theta) - \frac{ax}{2} \frac{\partial^2}{\partial Z^2} (y_{\text{F}} + y_{\text{O}} + \theta) = 0. \quad (2.21)$$

The boundary conditions for the conserved scalar can be determined from Eqs. (2.19) and (2.20) to be unity at both sides. Then with the unburnt state as initial condition, the solution of Eq. (2.21) is given by

$$y_{\text{F}} + y_{\text{O}} + \theta = 1. \quad (2.22)$$

Note that this particular choice of the initial condition does not restrict the solution since it is a requirement of every possible physical initial condition that it has to be realizable from the unburnt state. Since the non-dimensional product mass fraction y_{P} and temperature θ are governed by a mathematically similar flamelet equation (Eqs. (2.16) and (2.17)) and have the same boundary and initial conditions, it follows that

$$y_{\text{P}} = \theta, \quad (2.23)$$

which shows that Eq. (2.22) represents the mass conservation condition.

With Eq. (2.22) and the definition of the mixture fraction, Eq. (2.8), the mass fractions of fuel and oxidizer can be expressed in terms of mixture fraction and temperature as

$$y_{\text{O}} = 1 - Z - \frac{\nu}{\nu + 1} \theta = 1 - Z - (1 - Z_{\text{st}}) \theta \quad (2.24)$$

$$y_{\text{F}} = Z - \frac{\theta}{\nu + 1} = Z - Z_{\text{st}} \theta \quad (2.25)$$

and the chemical reaction rate, defined in Eq. (2.18), as

$$\omega = \text{Da} \frac{(1-\alpha) \exp(\beta_{\text{ref}} - \beta)}{1 - \alpha(1-\theta)} \left(\frac{Z}{Z_{\text{st}}} - \theta \right) \left(\frac{1-Z}{1-Z_{\text{st}}} - \theta \right) \exp \left(-Z e \frac{1-\theta}{1-\alpha(1-\theta)} \right). \quad (2.26)$$

With Eq. (2.26) the flamelet equation for the non-dimensional temperature given by Eq. (2.17) depends only on the temperature itself and can be integrated without solving the equations for the mass fractions of fuel, oxidizer, and product. If desired, these can be computed from Eqs. (2.23), (2.24), and (2.25).

2.4. Stochastic differential equations

In this section we want to derive an equation for the joint pdf of the temperature and the scalar dissipation rate. To complete Eq. (2.17) we need a stochastic differential equation (SDE) that governs the evolution of the scalar dissipation rate.

We consider a Stratonovich SDE given by Horsthemke & Lefever (1984)

$$d\chi_{\text{st}} = f(\chi_{\text{st}}) dt + \sigma \varphi(\chi_{\text{st}}) \circ dW(t), \quad (2.27)$$

where $W(t)$ denotes a Wiener process. In Eq. (2.27) the first term on the right-hand side is a drift term, the second a random term. The stationary probability density function corresponding to the Stratonovich SDE can be found to be

$$p_s(\chi_{\text{st}}) = \frac{N}{\sigma \varphi(\chi_{\text{st}})} \exp \left(\int_0^{\chi_{\text{st}}} \frac{2f(z)}{\sigma^2 \varphi^2(z)} dz \right). \quad (2.28)$$

It is well known that a good approximation for a stationary pdf of $\chi_{\text{st}}(t)$ is a lognormal distribution (Peters (1983)) given as

$$p_s(\chi_{\text{st}}) = \frac{1}{\chi_{\text{st}} \sqrt{2\pi\sigma^2}} \exp \left(-\frac{(\ln \chi_{\text{st}} - \ln \chi_{\text{st},0})^2}{2\sigma^2} \right), \quad (2.29)$$

from which it can easily be shown that the mean value of χ_{st} is

$$\bar{\chi}_{\text{st}} = \int_0^\infty \chi_{\text{st}} p_s(\chi_{\text{st}}) d\chi_{\text{st}} = \chi_{\text{st},0} \exp \left(\frac{\sigma^2}{2} \right). \quad (2.30)$$

To find $f(\chi_{\text{st}})$ and $\varphi(\chi_{\text{st}})$, one needs to equate Eqs. (2.29) and (2.28). From this we obtain

$$f(\chi_{\text{st}}) = -(\ln \chi_{\text{st}} - \ln \chi_{\text{st},0}) \frac{\chi_{\text{st}}}{t_\chi}, \quad \varphi(\chi_{\text{st}}) = \sqrt{\frac{2}{t_\chi}} \chi_{\text{st}}, \quad N = \frac{1}{\sqrt{\pi t_\chi}}. \quad (2.31)$$

For dimensional reasons a characteristic time scale t_χ has been introduced, which appears as a parameter of the problem. This time scale is associated with the time to reach a statistically stationary state. Therefore, it does not appear in the stationary pdf given by Eq. (2.29). The scalar dissipation rate $\chi(t)$ then obeys the following SDE

$$d\chi_{\text{st}} = -(\ln \chi_{\text{st}} - \ln \chi_{\text{st},0}) \frac{\chi_{\text{st}}}{t_\chi} dt + \sigma \sqrt{\frac{2}{t_\chi}} \chi_{\text{st}} \circ dW(t). \quad (2.32)$$

In non-dimensional form, this equation can be rewritten as

$$dx_{\text{st}} = -\frac{x_{\text{st}}}{\delta} \ln x_{\text{st}} d\tau + \sigma \sqrt{\frac{2}{\delta}} x_{\text{st}} \circ dW(\tau). \quad (2.33)$$

Here, $\delta = t_\chi \chi_{st,0}/a$ represents the ratio of the characteristic time scales of Eqs. (2.33) and (2.2). In a turbulent flow, the time scale t_χ would be modeled by the integral time scale of the turbulence or the scalar (Pope (2000)). Hence, t_χ can be expressed as

$$t_\chi = \frac{C_0 \overline{Z'^2}}{\chi_{st,0} \exp\left(\frac{\sigma^2}{2}\right)} \quad (2.34)$$

from which follows that

$$\delta = \frac{C_0 \overline{Z'^2}}{2\Delta Z \cdot Z_{st}(1 - Z_{st}) \exp\left(\frac{\sigma^2}{2}\right)}, \quad (2.35)$$

where C_0 is a constant and $\overline{Z'^2}$ is the mixture fraction variance. This shows that δ is independent of the mean scalar dissipation rate. Here, $\delta = 1$ will be assumed, which for $C_0 = 1$, $Z_{st} = 0.5$, and $\sigma = 1$ roughly corresponds to $Z' = 0.2$.

From a mathematical point of view, Eq. (2.17) with the source term Eq. (2.26) and the random scalar dissipation rate is a nonlinear stochastic partial differential equation, which can be solved but is very difficult to work with analytically. One way to analyze this equation is to derive the corresponding equation for the probability density functional for the temperature distribution $\theta(Z)$ (Fedotov (1992), Fedotov (1993)). However, since the random parameter $x(\tau, Z)$ appears in Eq. (2.17) as a multiplicative noise, it would be very difficult to obtain reasonable results. In order to simplify the problem, we will derive ordinary stochastic differential equations (SDE) for these quantities by modeling the diffusion term in Eq. (2.17).

It has been shown by Peters (1983) that these linear temperature profiles in the outer non-reactive structure can be found as the first order solution of an asymptotic analysis of the flamelet equations assuming one-step global chemistry. The assumption of linear temperature profiles in the outer structure will now be used for an approximation of the diffusion term appearing in Eq. (2.17).

The diffusion term evaluated at stoichiometric conditions can be written as a finite difference approximation over the reaction zone of width ΔZ as

$$\frac{\partial^2 T}{\partial Z^2} \Big|_{Z_{st}} \approx \frac{1}{\Delta Z} \left(\frac{\partial T}{\partial Z} \Big|^{+} - \frac{\partial T}{\partial Z} \Big|^{-} \right). \quad (2.36)$$

If the temperature gradients appearing in this expression are evaluated with the assumption of linear profiles in the non-reactive diffusion zones, the diffusion term can be approximated as

$$\frac{\partial^2 T}{\partial Z^2} \Big|_{Z_{st}} \approx -\frac{1}{\Delta Z} \left(\frac{T_{st} - T_1}{1 - Z_{st}} - \frac{T_2 - T_{st}}{Z_{st}} \right) = -\frac{T_{st} - T_{st,u}}{\Delta Z Z_{st} (1 - Z_{st})} = -\frac{(T_{st,b} - T_{st,u})}{\Delta Z Z_{st} (1 - Z_{st})} \theta_{st}. \quad (2.37)$$

Here, it has to be assumed that the reaction zone thickness ΔZ is independent of the scalar dissipation rate. Then, ΔZ is a constant which appears in the Damköhler number. The actual choice of ΔZ then only changes the value of the Damköhler number and is of no consequence for the conclusions of the paper. The validity of this assumption has been numerically evaluated by Cha (2000).

Introducing Eqs. (2.37) and (2.26) into Eq. (2.17) formulated at $Z = Z_{st}$ yields

$$\frac{d\theta_{st}}{d\tau} + x(\tau) \theta_{st} - \omega(\theta_{st}) = 0 \quad (2.38)$$

with

$$\omega = \text{Da} \frac{(1 - \alpha) \exp(\beta_{\text{ref}} - \beta)}{1 - \alpha(1 - \theta_{\text{st}})} (1 - \theta_{\text{st}})^2 \exp\left(-Z e \frac{1 - \theta_{\text{st}}}{1 - \alpha(1 - \theta_{\text{st}})}\right). \quad (2.39)$$

2.5. Joint probability density function

Now we are in a position to analyze how random fluctuations of the scalar dissipation rate can influence the non-premixed combustion process. It follows from Eqs. (2.38) and (2.33) that the pair process $(\theta_{\text{st}}(\tau), x_{\text{st}}(\tau))$ is Markovian, and therefore their probability density function $p = p(\tau, x_{\text{st}}, \theta_{\text{st}})$ is governed by the Fokker-Planck equation

$$\frac{\partial p}{\partial \tau} - \frac{1}{\delta} \frac{\partial}{\partial x_{\text{st}}} ((\ln x_{\text{st}} - \sigma^2) x_{\text{st}} p) + \frac{\partial}{\partial \theta_{\text{st}}} ((-x_{\text{st}} \theta_{\text{st}} + w(\theta_{\text{st}})) p) = \frac{\sigma^2}{\delta} \frac{\partial^2}{\partial x_{\text{st}}^2} (x_{\text{st}}^2 p) \quad (2.40)$$

with $0 < x_{\text{st}} < \infty$, $0 < \theta_{\text{st}} < 1$, and the boundary conditions

$$p(\tau, 0, \theta_{\text{st}}) = p(\tau, \infty, \theta_{\text{st}}) = p(\tau, x_{\text{st}}, 0) = p(\tau, x_{\text{st}}, 1) = 0. \quad (2.41)$$

It is convenient to introduce the natural logarithm of the stoichiometric scalar dissipation rate as a new independent variable

$$x_{\text{ln}} = \ln x_{\text{st}}. \quad (2.42)$$

The pdf of x_{ln} can then be obtained by the normalization condition

$$p(x_{\text{st}}) = \frac{p_{\text{ln}x}}{x_{\text{st}}} \quad (2.43)$$

and Eq. (2.40) can be written as

$$\frac{\partial p_{\text{ln}x}}{\partial \tau} - \frac{1}{\delta} \frac{\partial}{\partial x_{\text{ln}}} (x_{\text{ln}} p_{\text{ln}x}) + \frac{\partial}{\partial \theta_{\text{st}}} ((-e^{x_{\text{ln}}} \theta_{\text{st}} + \omega) p_{\text{ln}x}) - \frac{\sigma^2}{\delta} \frac{\partial^2 p_{\text{ln}x}}{\partial x_{\text{ln}}^2} = 0. \quad (2.44)$$

The boundary conditions are given by

$$p_{\text{ln}x}(\tau, -\infty, \theta_{\text{st}}) = p_{\text{ln}x}(\tau, \infty, \theta_{\text{st}}) = p_{\text{ln}x}(\tau, x_{\text{ln}}, 0) = p_{\text{ln}x}(\tau, x_{\text{ln}}, 1) = 0. \quad (2.45)$$

Note that, as shown by Eq. (2.43), the distribution $p_{\text{ln}x}$ is different from p and the maximum will in general be at a different value of the scalar dissipation rate. However, since both functions can easily be converted into each other, the conclusions do not depend on the choice of the formulation used for the analysis.

3. Numerical solution

Equation (2.44) has been solved numerically using a 4th order Runge-Kutta scheme with adaptive step-size control. The convection term in the x_{ln} -direction has been discretized using central differences, the convection term in the θ_{st} -direction by a robust, globally second order upwind scheme as given by Koren (1996). The equations are solved on a 300×300 equidistant grid. The numerical time-step is restricted by a CFL condition which is imposed by the high convection velocity in the θ_{st} -direction at high scalar dissipation rate. This can be observed in Fig. 2, which will be described below. The initialization is performed with a numerical δ -function at some point in the $x_{\text{ln}}-\theta_{\text{st}}$ -space.

4. Results and discussion

In this section we will first provide a general discussion of Eq. (2.44) and the parameters Da , Ze , and α appearing in this equation. Numerical solutions of Eq. (2.44) will then be presented for a variation of the scalar dissipation rate variance σ , and the results will be discussed.

Numerical solutions of Eq. (2.44) will then be presented. The results for different values of the scalar dissipation rate variance σ will be discussed.

4.1. General discussion

Equation (2.44) is a two-dimensional unsteady partial differential equation depending on x_{ln} and θ_{st} . In the direction of x_{ln} , the equation reveals a convective term and a diffusion term. The convective term describes the relaxation to the mean. The mean value is achieved when the convection velocity is zero. This implies that the mean value of the non-dimensional scalar dissipation rate is $x_{\text{ln}} = 0$, which follows trivially from the normalization of χ_{st} . However, it is interesting to note that only the scalar dissipation rate itself determines the speed at which it relaxes to its mean. The diffusion term describes the broadening of the pdf by fluctuations of the scalar dissipation rate with σ^2 appearing as the diffusion coefficient.

In the direction of θ_{st} , Eq. (2.44) only reveals a convection term. Setting the convection velocity $V_{\theta_{\text{st}}} = -e^{x_{\text{ln}}}\theta_{\text{st}} + \omega$ equal to zero yields the steady state relation between the temperature and the scalar dissipation rate in the absence of scalar dissipation rate fluctuations as

$$x(\theta_{\text{st}}) = Da \exp\left(\left.\frac{Ze}{\alpha}\right|_{\text{ref}} - \frac{Ze}{\alpha}\right) \frac{(1-\alpha)(1-\theta_{\text{st}})^2}{\theta_{\text{st}}(1-\alpha(1-\theta_{\text{st}}))} \exp\left(-Ze\frac{1-\theta_{\text{st}}}{1-\alpha(1-\theta_{\text{st}})}\right). \quad (4.1)$$

This relation describes the so called S-shaped curve for non-premixed combustion (Peters (1984)), which depends on three parameters: the Damköhler number Da , the Zeldovich number Ze , and the heat release parameter α , where Ze and α only depend on the chemistry.

Figure 1 shows S-shaped curves from solutions of Eq. (4.1) for different values of these parameters[†]. It is well known and will be shown in the following discussion that stable solutions can only be achieved for the upper and the lower branch, whereas solutions given by the middle branch are unstable. Considering the fact that the S-shaped curves shown in Fig. 1 represent states with zero convection velocity in the direction of θ_{st} , it can be seen from Eq. (2.44) that the convection velocity $V_{\theta_{\text{st}}}$ is positive for scalar dissipation rates smaller than $x_{\text{ln}}(\theta_{\text{st}})$ as given from Eq. (4.1) and negative for larger values. The consequence is that the convection velocity in the θ -direction is always directed away from the intermediate branch, which shows that these solutions are unstable. It also shows that starting from an unburnt solution, the scalar dissipation rate has to be decreased below the value at the lower turning point of the curve to be able to auto-ignite. This value will, therefore, be referred to as ignition scalar dissipation rate x_{ig} . Correspondingly, starting from a burning solution, the flame can only be extinguished by increasing the scalar dissipation rate over the value at the upper turning point. This value will, therefore, be called extinction scalar dissipation rate x_{ex} .

For non-premixed methane flames, the activation energy of a one-step global reaction

[†] For constant scalar dissipation rate this relation would be plotted as function of the Damköhler number, which would be proportional to x_{ln}^{-1} . In the present paper these curves are plotted over x_{ln} and therefore mirrored. However, we still use the phrase S-shaped curve.

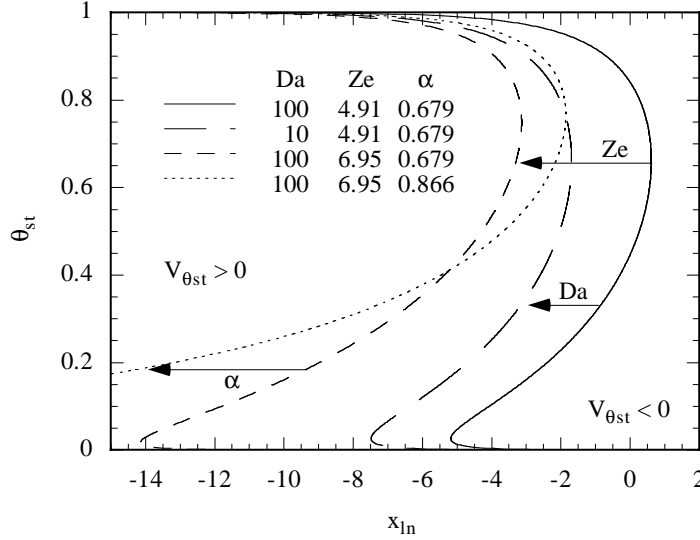


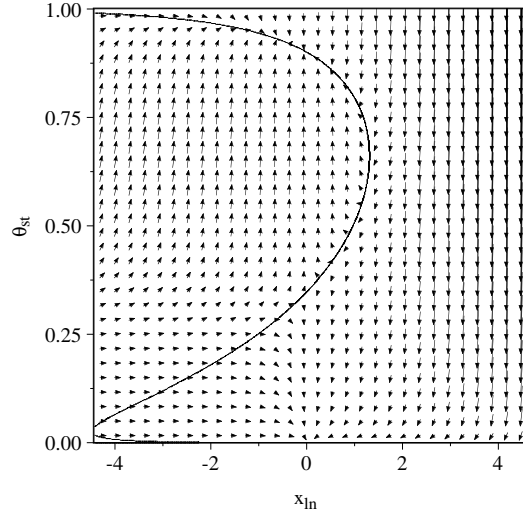
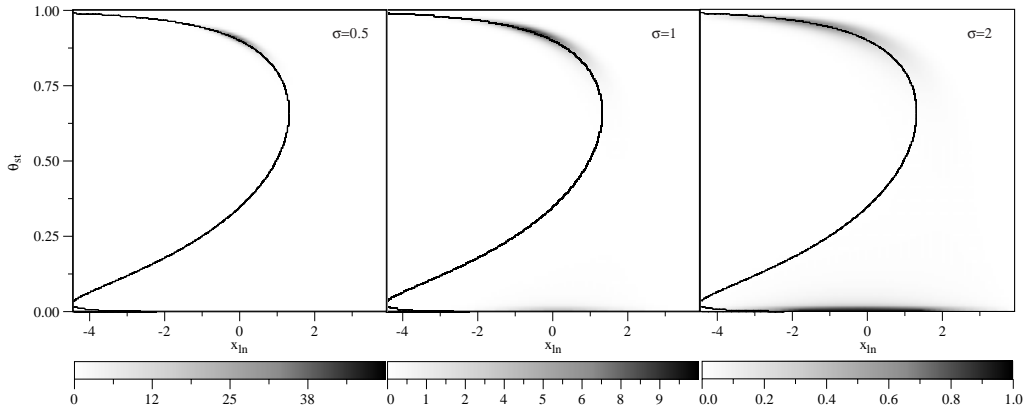
FIGURE 1. S-shaped curve determined from Eq. (4.1) for different parameter variations. Parameter changes are indicated by arrows.

can be assumed to be $E = 150 \text{ kJ/kg}$ (Seshadri (1999)). This implies a value of $\beta_{\text{ref}} = 8.03$ for a methane/air-system at ambient conditions. Then, the solid line in Fig. 1 corresponds to a case with preheated air at $T_2 = 800 \text{ K}$ and the dotted line to an air temperature of $T_2 = 300 \text{ K}$. For both cases the fuel temperature is assumed to be $T_1 = 300 \text{ K}$ and the pressure to be 1 bar. It is clear from Eq. (4.1) and it can be seen in Fig. 1 that a variation in the Damköhler number simply shifts the curve. In contrast, a variation of the Zeldovich number leads to moderately lower scalar dissipation rate for extinction and a strongly decreased ignition scalar dissipation rate.

The strongest influence however, can be seen by changing the heat release parameter. Although by increasing α the extinction scalar dissipation rate is only slightly increased, the ignition scalar dissipation rate is decreased very strongly to a value of approximately $x_{\text{in,ig}} \approx -40$ corresponding to $x_{\text{ig}} \approx 10^{-17}$ for the example shown in Fig. 1. This merely shows that auto-ignition of methane at ambient conditions is almost impossible.

Figure 2 shows a two-dimensional vector representation of the velocities of particles in the $\theta_{\text{st}}-x_{\text{in}}$ space, where the term particle is defined by a point and the associated velocity in this space. This figure again clearly shows that the pdf tends to move to $x_{\text{in}} = 0$ and generally away from the unstable branch. However, at low temperature and low scalar dissipation rate on the left side of the S-shaped curve, for instance, the driving force in the direction of the mean scalar dissipation rate is so strong that particles might cross the unstable branch. Even though these particles were initially in a regime which would for constant x_{in} lead to ignition, these particles will then be attracted by the lower branch.

In the present example this effect is not so obvious for particles originating from a burning state with a scalar dissipation rate higher than the extinction limit, which would be located in the upper right corner in Fig. 2. These particles can also change during the extinction process to lower scalar dissipation rates and might cross the S-shaped curve. This would lead to a recovery to the burning state. It has been discussed before and is indicated in Fig. 1 that, in the absence of scalar dissipation rate changes, all particles on the left side of the unstable branch of the S-shaped curve will change to the burning

FIGURE 2. Convection velocities in θ_{st} - x_{in} space.FIGURE 3. Calculated joint θ_{st} - x_{in} probability density function at $\tau = 5$.

state, whereas particles on the right will change to the non-burning state. However, it has clearly been demonstrated here that this is different in the case of a fluctuating scalar dissipation rate, where the unstable branch does not uniquely separate these two regimes.

4.2. Numerical results

For the numerical solution of the equation for the joint pdf of θ_{st} and x_{in} , Eq. (2.44), the parameters appearing in this equation have been set to $Da = 200$, $Ze = 4.91$, and $\alpha = 0.679$. As mentioned above, this corresponds to a methane/air-system, where the air is preheated to $T_2 = 800$ K. Results of the numerical simulations at time $\tau = 5$ are presented exemplarily for $\sigma = 1$ in Fig. 3. All calculations have been started with a δ -function at $\theta_{st} = 0.9$ and $x_{in} = 0$ as initial condition for the probability density function, which is then given by $p(\tau = 0, x_{in}, \theta_{st}) = \delta(x_{in}, \theta_{st} - 0.9)$.

The joint pdfs of θ_{st} and x_{in} are given in Fig. 3 for different values of the scalar dissipation rate variance σ . It can be observed that even for the low variance case $\sigma =$

0.5, the distribution of high probability density is already rather broad, extending from approximately $-1 < x_{\text{ln}} < 1$ and mainly around the upper branch of the S-shaped curve. Even though this cannot be seen in Fig. 3, the numerical results show that there is already some probability to find the extinguished state around $x_{\text{ln}} = 0$.

It follows from the above discussion that extinguished particles originate from burning particles, which, because of the fluctuations of the scalar dissipation rate, have experienced a scalar dissipation rate high enough to completely extinguish the particle without crossing the unstable branch of the S-shaped curve. This would result in re-ignition. The low probability of finding these high scalar dissipation rates then forces the extinguished particles to a state around $x_{\text{ln}} = 0$. In a real turbulent diffusion flame, these extinguished areas could re-ignite by heat conduction from the surrounding, still burning gas. This effect, however, is not included in the current analysis. Therefore, re-ignition can only occur here if the scalar dissipation rate of an extinguished particle becomes smaller than the ignition limit. This, however, is prohibited in the present simulations by choosing the lower boundary for x_{ln} larger than the ignition scalar dissipation rate. This allows study of the extinction process without the influence of auto-ignition.

It is important to recognize that because of this assumption the steady state solution is always completely non-burning. This means that, for this dynamic system scalar dissipation rate, fluctuations even of small amplitude lead to a phase transition from the burning to the non-burning state. This dynamical character would not be observed in the deterministic case.

For $\sigma = 1$ the distribution is even broader, revealing substantial probability for $-2 < x_{\text{ln}} < 2$. Also, the probability of finding extinguished states is already of comparable magnitude as for the burning states. As for $\sigma = 0.5$ the region of high probability is still concentrated around the S-shaped curve, indicating that the chemistry is fast enough to compensate scalar dissipation rate fluctuations. It is also interesting to note that similar to the findings of Oberlack *et al.* (1999) there is only a very low probability of finding states between burning and extinguished. This shows that the extinction process is fast compared to other time scales of the system.

The solution for an even larger scalar dissipation rate variance of $\sigma = 2$ shows that the probability distribution is further broadened and the fraction of extinguished states is even higher. Most interesting here is the observation that, particularly at high scalar dissipation rates close to extinction, the high probability region clearly departs from the S-shaped curve. This can also be observed in Fig. 3 but to a smaller extent. The departure from the S-shaped curve indicates that the chemistry is not fast enough to relax the temperature in accordance with large scale scalar dissipation rate fluctuations to the steady solution. At low scalar dissipation rate, the high probability region is still very close to the S-shaped curve.

5. Conclusions and future work

In the present work the flamelet equations have been formulated for a one-step global reaction and used for the investigation of the influence of scalar dissipation rate fluctuations on non-premixed turbulent combustion. By modeling the diffusion term in the flamelet equation, ordinary stochastic differential equations were derived for the temperature and the scalar dissipation rate at stoichiometric mixture. From these, a Fokker-Planck equation for the joint probability density function of temperature and the scalar

dissipation rate has been derived. The equation has been discussed and numerical solutions for varying scalar dissipation rate variance provided.

The analysis shows that the S-shaped curve, which represents the steady-state solution for a given scalar dissipation rate in the absence of scalar dissipation rate fluctuations, separates the $\theta_{\text{st}}-x_{\text{ln}}$ space into two regimes, which will either lead to the burning or the extinguished state. It is also shown that scalar dissipation rate fluctuations even of small amplitude will under the present simplifications cause a phase transition from the burning to the completely extinguished state.

Numerical solutions show an increasing fraction of extinguished states for increasing scalar dissipation rate variance at a given time. It is also found that particles with a scalar dissipation rate higher than the extinction limit can recover to a burning solution during the extinction process. Therefore, for a fluctuating scalar dissipation rate, particles can cross the S-shaped curve, which thereby no longer separates regimes that uniquely lead to the extinguished or the burning state.

Furthermore, it is found that the low probability of finding high scalar dissipation rate forces particles which have been extinguished at high scalar dissipation rate to rapidly change to a state with lower scalar dissipation rate, where re-ignition could occur. For higher scalar dissipation rate variance it is observed that the high probability region clearly departs from the S-shaped curve. This indicates that the chemistry is not fast enough to relax large scale scalar dissipation rate fluctuations to the steady state solution. This has been shown to have an important implication in the application of flamelet type models in non-premixed turbulent combustion.

The presented method has been shown to provide a useful tool to study the effect of random scalar dissipation rate fluctuations. In future work, the model is to be corroborated with results from direct numerical simulations of turbulent reacting flows and the re-ignition process is to be included. The investigation of the influence of scalar dissipation rate fluctuations on auto-ignition delay times and pollutant formation could also be a worthwhile extension of the present work.

Acknowledgments

The authors gratefully acknowledge funding by the US Department of Energy in the frame of the ASCI program and the Center for Turbulence Research. We are indebted to Chong Cha for many inspiring discussions and for providing solutions of Monte Carlo simulations for the investigated problem.

REFERENCES

- BARLOW, R. S. & CHEN, J.-Y. 1992 On transient flamelets and their relationship to turbulent methane-air jet flames. *Proc. Combust. Inst.* **24**, 231-237.
- BARTHS, H., PETERS, N., BREHM, N., MACK, A., PFITZNER, M. & SMILJANOVSKI, V. 1998 Simulation of pollutant formation in a gas turbine combustor using unsteady flamelets. *Proc. Combust. Inst.* **27**, 1841-1847.
- BUYEVICH, Y. A., FEDOTOV, S. P. & TRET'YAKOV, M. V. 1993 Heterogeneous reaction affected by external noise. *Physica A.* **198**, 354-367.
- CHA, C. M. 2000 Private communication.
- FEDOTOV, S. P. 1992 Statistical model of the thermal ignition of a distributed system. *Comb. Flame.* **91**, 65-70.

- FEDOTOV, S. P. 1993 Stochastic analysis of the thermal ignition of a distributed explosive system. *Phys. Lett. A* **176**, 220-224.
- HAWORTH, D., C., DRAKE, M., C., POPE, S., B. & BLINT, R., J. 1988 The importance of time-dependent flame structures in stretched laminar flamelet models for turbulent jet diffusion flames. *Proc. Combust. Inst.* **22**, 589-597.
- HORSTHEMKE, W. & LEFEVER, R. 1984 *Noise-Induced Transitions*, Springer-Verlag.
- KLIMENKO, A. Y. & BILGER, R. W. 1999 Conditional moment closure for turbulent combustion. *Prog. Energy Combust. Sci.* **25**, 595-687.
- KOREN, B. 1996 A robust upwind discretization method for advection, diffusion and source terms. in C. B. Vreugdenhil & B. Koren (eds). *Numerical methods for advection-diffusion problems*, Vol. 45 of *Notes on Numerical Fluid Dynamics*, Vieweg Verlag, Braunschweig.
- KUZNETSOV, V. R. & SABEL'NIKOV, V. A. 1990 *Turbulence and Combustion*, Hemisphere Publishing Corp.
- MAUSS, F., KELLER, D. & PETERS, N. 1990 A lagrangian simulation of flamelet extinction and re-ignition in turbulent jet diffusion flames. *Proc. Combust. Inst.* **23**, 693-698.
- OBERLACK, M., ARLITT, R. & PETER, N. 1999 On stochastic Damköhler number variations in a homogeneous flow reactor. *Comb. Theory Modeling*, submitted.
- O'BRIEN, E. E. 1980 The probability density function (pdf) approach to reacting turbulent flows. in L. P. A. & F. A. Williams (eds). *Turbulent Reacting Flows*, Springer Verlag, pp. 185-218.
- PETERS, N. 1983 Local quenching due to flame stretch and non-premixed turbulent combustion. *Combust. Sci. Technol.* **30**, 1.
- PETERS, N. 1984 Laminar diffusion flamelet models in non-premixed turbulent combustion. *Prog. Energy Combust. Sci.* **10**, 319-339.
- PETERS, N. 1987 Laminar flamelet concepts in turbulent combustion. *Proc. Combust. Inst.* **21**, 1231-1250.
- PITSCH, H., BARTHS, H. & PETERS, N. 1996 Three-dimensional modeling of nox and soot formation in di-diesel engines using detailed chemistry based on the interactive flamelet approach. *SAE Paper 962057*.
- PITSCH, H., CHEN, M. & PETERS, N. 1998 Unsteady flamelet modeling of turbulent hydrogen/air diffusion flames. *Proc. Combust. Inst.* **27**, 1057-1064.
- PITSCH, H. & STEINER, H. 2000 Large-eddy simulation of a turbulent piloted methane/air diffusion flame (Sandia flame D). *Phys. Fluids*, submitted.
- PITSCH, H., WAN, Y. P. & PETERS, N. 1995 Numerical investigation of soot formation and oxidation under diesel engine conditions. *SAE Paper 952357*.
- POPE, S. B. 1985 Pdf methods for turbulent reactive flows. *Prog. Energy Combust. Sci.* **11**, 119.
- POPE, S. B. 2000 *Turbulent Flows*, Cambridge University Press, chapter 12.
- SAITOH, T. & OTSUKA, Y. 1976 Unsteady behavior of diffusion flames and premixed flames for count flow geometry. *Combust. Sci. Tech.* **12**, 135-146.
- SESHADRI, K. 1999 Rate-ratio asymptotics applied to flames. Paper presented at the Western States Section of the Combustion Institute, Fall 1999 Meeting, University of California at Irvine, Irvine, California.